PAPER • OPEN ACCESS

Quenching of bright and dark excitons via deep states in the presence of SRH recombination in 2D monolayer materials

To cite this article: Jdrzej Szmytkowski 2023 *J. Phys.: Condens. Matter* **35** 015601

View the article online for updates and enhancements.

Quenching of bright and dark excitons via deep states in the presence of SRH recombination in 2D monolayer materials

Jędrzej Szmytkowski

Faculty of Applied Physics and Mathematics, Gdańsk University of Technology, Narutowicza 11/12, 80-233 Gdańsk, Poland

E-mail: jedszmyt@pg.edu.pl

Abstract

Two-dimensional (2D) monolayer materials are interesting systems due to an existence of optically non-active dark excitonic states. In this work, we formulate a theoretical model of an excitonic Auger process which can occur together with the trap-assisted recombination in such 2D structures. The interactions of intravalley excitons (bright and spin-dark ones) and intervalley excitons (momentum-dark ones) with deep states located in the energy midgap have been taken into account. The explanation of this process is important for the understanding of excitonic and photoelectrical processes which can coexist in 2D materials, like transition metal dichalcogenides and perovskites.

Keywords: 2D materials, excitons, recombination

(Some figures may appear in colour only in the online journal)

1. Introduction

In recent years, two-dimensional (2D) monolayer materials are widely studied due to their unusual excitonic properties in comparison to traditional three-dimensional (3D) structures. For atomically thin layers, we can distinguish bright and dark excitons. The formation of bright excitonic states occurs by the spin-allowed optical absorption inside the same valley. However, one can find also a different type of the intravalley exciton, where an electron and a hole are Coulomb-bound by the transition which is optically forbidden. For this case, we say about a spin-forbidden dark excitonic state. Due to

multiple maxima and minima in the electronic structure of 2D materials, there is a possibility to form an exciton which consists of an electron and a hole located in different valleys. Such an intervalley excitonic state can be treated as a momentum-forbidden dark exciton [1–9].

Atomically thin materials, like transition metal dichalcogenides, are considered as promising candidates to produce an efficient radiative recombination in optoelectronic and photonic devices [3]. However, the existence of dark excitons leads to decreasing of the luminescence efficiency. Recently, a great attention has been focused on the usage of hybrid organic–inorganic perovskites in photovoltaics and in light-emitting diodes. Also for perovskites, it is possible to fabricate thin 2D structures [10–12]. Therefore, a role of excitonic states and their influence on photoelectric effects should be fully understood.

During the growth process of 2D structures, many defects can be created (vacancies, dislocations or impurities) [13].

Some defects are responsible for an induction of midgap states which serve as recombination centers for separated electrons and holes. If a recombination via such a channel occurs, we say about the trap-assisted or the Shockley–Read–Hall (SRH) recombination [14, 15]. Recently, the recombination of charge carriers through defects has been observed in 2D materials [16, 17]. In addition, excitons can also be trapped by the defect states in such atomically thin structures [18].

Another possible type of charge carriers recombination is based on a three body Auger process. It has been shown that such a phenomenon can coexist together with the SRH recombination [19]. Also excitonic processes can be of the Auger type. An excitonic Auger (EA) recombination via deep states located in the midgap has been proposed to explain experimental results for silicon [20]. Recently, this EA mechanism has been discussed for 2D materials [21]. It should be mentioned that the EA recombination process via deep states is different than a previously proposed effect, called the phonon-assisted Auger recombination of excitons, which can also occur in monolayer structures [22].

Recently, a coexistence of both the EA and the SRH processes has been theoretically considered for 3D materials [23] and for organic semiconductors [24]. In the case of photo-electrical and optoelectronic devices based on 2D materials, it is required to explain all possible mechanisms which influence both the recombination process of charge carriers and the quenching of excitons. Therefore, the aim of this work is to take into account the EA recombination of intravalley and intervalley excitons which can occur together with the SRH recombination. It should give a deeper insight into the electrical and excitonic properties of monolayer structures.

2. Model

In the following, first we will briefly remind the well-known SRH recombination of separated charge carriers [14, 15]. Next, the theoretical model of the SRH process combined with the EA recombination mechanism is formulated for bright and dark excitons in 2D structures. Here, we will use shorter names to construct abbreviations for dark excitons (without the word 'forbidden'): spin-dark (SD) exciton and momentum-dark (MD) exciton.

2.1. The SRH recombination

In the trap-assisted recombination model, free charge carriers are captured by deep states which are located in the energy band-gap. Let us assume that n and p are concentrations of electrons in the conduction band and holes in the valence band, respectively. We can define the capture rates E_{cap} for electrons and H_{cap} for holes as

$$E_{\text{cap}} = C_n n N_t (1 - f) \tag{1}$$

and

$$H_{\text{cap}} = C_p p N_t f, \tag{2}$$

where parameters C_n and C_p are probabilities of the capture processes (capture coefficients) for electrons and holes, respectively, N_t represents a concentration of deep trap states in the midgap and the parameter f describes the function which informs about a probability that electrons occupy deep states.

Both types of charge carriers can be emitted from deep traps to the conduction or to the valence band. The rates which characterize such emission processes E_{em} (for electrons) and H_{em} (for holes) can be written as

$$E_{\text{em}} = C_n n_1 N_t f \tag{3}$$

and

$$H_{\text{em}} = C_p p_1 N_t (1 - f). \tag{4}$$

Here, the concentrations for electrons n_1 and holes p_1 describe a case when the trap level E_t has the same position as the Fermi level E_F. These concentrations are defined as

$$n_1 = N_c \exp\left(-\frac{E_c - E_t}{kT}\right) \tag{5}$$

and

$$p_1 = N_v \exp\left(-\frac{E_t - E_v}{kT}\right), \tag{6}$$

where the parameters N_c and N_v are the effective densities of states associated with the conduction and the valence bands, respectively, the energies E_c and E_v denote positions of the edges for both bands, k represents the Boltzmann constant and T is the absolute temperature.

The recombination rate to describe the trap-assisted type of recombination is given by [14, 15]

$$U_{\text{SRH}} = \frac{np - n_{\text{int}}^2}{\tau_p(n + n_1) + \tau_n(p + p_1)}, \tag{7}$$

where the intrinsic concentration of charge carriers is defined as

$$n_{\text{int}} = (N_c N_v)^{1/2} \exp\left(-\frac{E_g}{2kT}\right). \tag{8}$$

Here, E_g represents the bandgap energy, whereas the parameters $\tau_n = 1/(N_t C_n)$ and $\tau_p = 1/(N_t C_p)$ denote the lifetimes of electrons (n) and holes (p), respectively.

2.2. The EA mechanism combined with the SRH recombination

Excitons can also interact with deep states. In the EA mechanism [23], the charge carrier from an exciton is captured by a deep trap and, as a consequence, the opposite sign carrier is emitted from the same exciton to the exciton continuum (which can be treated as the band for separated electrons or holes). Therefore, these capture and emission processes are not independent. For 2D materials, three types of excitons (bright, SD and MD) can participate in such an Auger-type excitonic
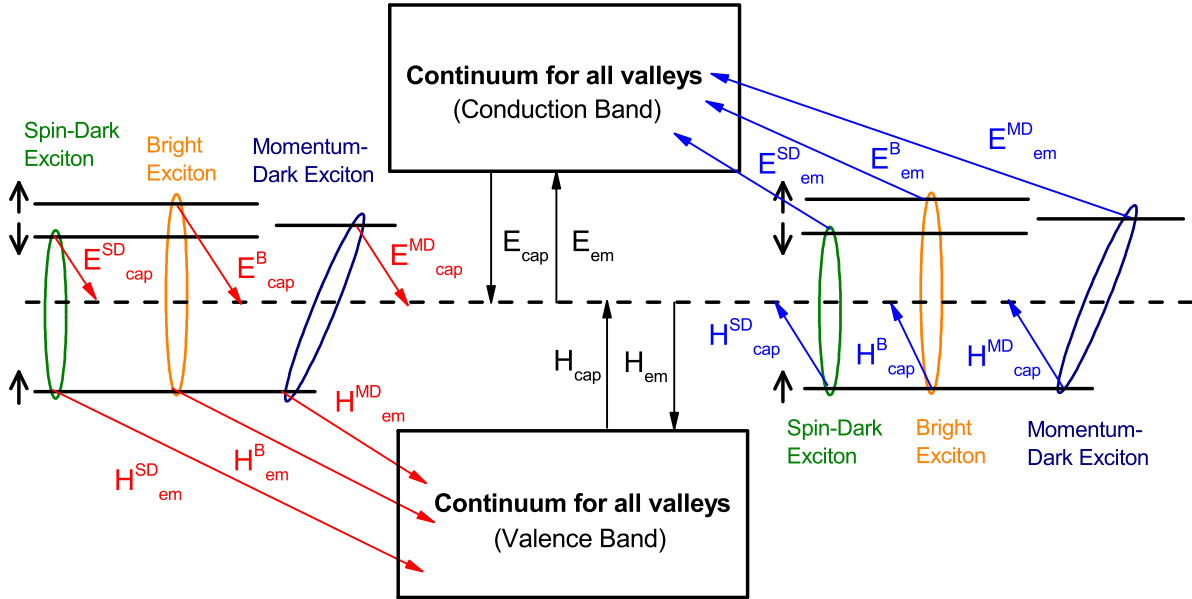
Figure 1. A diagram of all charge carriers transitions which occur in the presented EA and SRH mechanisms.

phenomenon. Figure 1 shows a schematic diagram of all transitions which take part in both the EA mechanism and the SRH recombination.

The rates for the capture of electrons from bright excitons ($E_{\text{cap}}^{\text{B}}$), SD excitons ($E_{\text{cap}}^{\text{SD}}$) and MD excitons ($E_{\text{cap}}^{\text{MD}}$), which are equal to the emission rates of holes from bright excitons (H_{em}^{B}), SD excitons ($H_{\text{em}}^{\text{SD}}$) and MD excitons ($H_{\text{em}}^{\text{MD}}$), respectively, can be defined as

$$E_{\text{cap}}^{\text{B}} = A_{\text{B}}^{(n)} X_{\text{B}} N_t (1 - f) = H_{\text{em}}^{\text{B}}, \tag{9}$$

$$E_{\text{cap}}^{\text{SD}} = A_{\text{SD}}^{(n)} X_{\text{SD}} N_t (1 - f) = H_{\text{em}}^{\text{SD}} \tag{10}$$

and

$$E_{\text{cap}}^{\text{MD}} = A_{\text{MD}}^{(n)} X_{\text{MD}} N_t (1 - f) = H_{\text{em}}^{\text{MD}}, \tag{11}$$

where $A_{\text{B}}^{(n)}$, $A_{\text{SD}}^{(n)}$ and $A_{\text{MD}}^{(n)}$ represent probabilities of capture processes for electrons (capture coefficients) from bright excitons, SD excitons and MD excitons, respectively, whereas the parameters X_{B}, X_{SD} and X_{MD} denote concentrations of bright excitons, SD excitons and MD excitons, respectively.

Now, we consider the capture of holes from excitonic states. For the Auger excitonic mechanism, they are associated with the emission processes of electrons from the same excitons. Therefore, the capture rates of holes from bright excitons ($H_{\text{cap}}^{\text{B}}$), SD excitons ($H_{\text{cap}}^{\text{SD}}$) and MD excitons ($H_{\text{cap}}^{\text{MD}}$) are equal to electron emission rates from bright excitons (E_{em}^{B}), SD excitons ($E_{\text{em}}^{\text{SD}}$) and MD excitons ($E_{\text{em}}^{\text{MD}}$), respectively. We can write

$$H_{\text{cap}}^{\text{B}} = A_{\text{B}}^{(p)} X_{\text{B}} N_t f = E_{\text{em}}^{\text{B}}, \tag{12}$$

$$H_{\text{cap}}^{\text{SD}} = A_{\text{SD}}^{(p)} X_{\text{SD}} N_t f = E_{\text{em}}^{\text{SD}} \tag{13}$$

and

$$H_{\text{cap}}^{\text{MD}} = A_{\text{MD}}^{(p)} X_{\text{MD}} N_t f = E_{\text{em}}^{\text{MD}}, \tag{14}$$

where the capture coefficients $A_{\text{B}}^{(p)}$, $A_{\text{SD}}^{(p)}$ and $A_{\text{MD}}^{(p)}$ denote probabilities of a capture of holes from bright excitons, SD excitons and MD excitons, respectively.

Next, we take into account kinetic equations which describe a change of the excitons concentrations in time (t). There can be several phenomena leading to the creation and the decay of intravalley and intervalley excitonic states which are not related to our model. For convenience, we write all rates for these processes as the sums of different generation and decay channels. Thus, the kinetic equations can be written as

$$\frac{\partial X_{\text{B}}}{\partial t} = \sum_i G_i^{\text{B}} - \sum_i R_i^{\text{B}} - E_{\text{cap}}^{\text{B}} - H_{\text{cap}}^{\text{B}}, \tag{15}$$

$$\frac{\partial X_{\text{SD}}}{\partial t} = \sum_i G_i^{\text{SD}} - \sum_i R_i^{\text{SD}} - E_{\text{cap}}^{\text{SD}} - H_{\text{cap}}^{\text{SD}} \tag{16}$$

and

$$\frac{\partial X_{\text{MD}}}{\partial t} = \sum_i G_i^{\text{MD}} - \sum_i R_i^{\text{MD}} - E_{\text{cap}}^{\text{MD}} - H_{\text{cap}}^{\text{MD}}, \tag{17}$$

where G_i^{B}, G_i^{SD} and G_i^{MD} are the generation rates for bright excitons, SD excitons and MD excitons, respectively, whereas R_i^{B}, R_i^{SD} and R_i^{MD} denote the decay rates for bright excitons, SD excitons and MD excitons, respectively.

We can also write the kinetic equations for populations of electrons and holes. Analogically to the previous case presented for excitons, all processes of generation or decay not related to our model are written with the sum notation. Thus, we obtain

$$\frac{\partial n}{\partial t} = \sum_i G_i^{(n)} - \sum_i R_i^{(n)} - U_n \tag{18}$$

and

$$\frac{\partial p}{\partial t} = \sum_i G_i^{(p)} - \sum_i R_i^{(p)} - U_p, \qquad (19)$$

where $G_i^{(n)}$ and $G_i^{(p)}$ denote the generation rates for electrons and holes, respectively, whereas $R_i^{(n)}$ and $R_i^{(p)}$ are the recombination (or decay) rates for electrons and holes, respectively.

In the above equations, the recombination rates via deep states for separated charge carriers are given by

$$U_n = E_{cap} - E_{em} - E_{em}^B - E_{em}^{SD} - E_{em}^{MD} \qquad (20)$$

for electrons and

$$U_p = H_{cap} - H_{em} - H_{em}^B - H_{em}^{SD} - H_{em}^{MD} \qquad (21)$$

for holes. Here, we should remind that the emission of a charge carrier from the exciton to a continuum state occurs simultaneously with the transfer of an opposite sign carrier from the same exciton to a deep trap. Therefore, both these transitions are treated as the same process. In addition, there is an assumption that other processes written with sums in equations (15)–(19) do not require deep traps. For steady state conditions, we can write that $U_n = U_p = U$.

The trap occupancy functions look as follows

$$f = \left(C_n n + C_p p_1 + A_B^{(n)} X_B + A_{SD}^{(n)} X_{SD} + A_{MD}^{(n)} X_{MD} \right)$$
$$\times \left[C_n(n+n_1) + C_p(p+p_1) + \left(A_B^{(n)} + A_B^{(p)} \right) X_B \right.$$
$$\left. + \left(A_{SD}^{(n)} + A_{SD}^{(p)} \right) X_{SD} + \left(A_{MD}^{(n)} + A_{MD}^{(p)} \right) X_{MD} \right]^{-1} \qquad (22)$$

for electrons and

$$1-f = \left(C_n n_1 + C_p p + A_B^{(p)} X_B + A_{SD}^{(p)} X_{SD} + A_{MD}^{(p)} X_{MD} \right)$$
$$\times \left[C_n(n+n_1) + C_p(p+p_1) + \left(A_B^{(n)} + A_B^{(p)} \right) X_B \right.$$
$$\left. + \left(A_{SD}^{(n)} + A_{SD}^{(p)} \right) X_{SD} + \left(A_{MD}^{(n)} + A_{MD}^{(p)} \right) X_{MD} \right]^{-1} \qquad (23)$$

for the case of holes.

Now, we can find the formula which describes the effective recombination rate of the SRH recombination which coexists with the EA process in the form

$$U = \frac{n^* p^* - n_{int}^2}{\tau_p^* \left(n^* + n_1 \right) + \tau_n^* \left(p^* + p_1 \right)}. \qquad (24)$$

Here, the parameters n^* and p^* can be treated as effective concentrations. We obtain that

$$n^* = \frac{n\, C_n n_1}{C_n n_1 + A_B^{(p)} X_B + A_{SD}^{(p)} X_{SD} + A_{MD}^{(p)} X_{MD}} \qquad (25)$$

and

$$p^* = \frac{p\, C_p p_1}{C_p p_1 + A_B^{(n)} X_B + A_{SD}^{(n)} X_{SD} + A_{MD}^{(n)} X_{MD}}. \qquad (26)$$

The quantities τ_n^* and τ_p^* have forms

$$\tau_n^* = \frac{n_1}{N_t \left(C_n n_1 + A_B^{(p)} X_B + A_{SD}^{(p)} X_{SD} + A_{MD}^{(p)} X_{MD} \right)} \qquad (27)$$

and

$$\tau_p^* = \frac{p_1}{N_t \left(C_p p_1 + A_B^{(n)} X_B + A_{SD}^{(n)} X_{SD} + A_{MD}^{(n)} X_{MD} \right)}. \qquad (28)$$

Apart from the simple situation with one type of bright exciton and two types of dark excitons (spin- and momentum-forbidden ones), one can expect an existence of more kinds of intravalley and intervalley excitonic states which are associated with the exact electronic structure of 2D materials. For example, many combinations of MD excitons have been recently found for WX_2 and MX_2 dichalcogenides [6] where holes from dark excitons can be located in different valleys. Considering such a case, it is easy to derive that then we should replace terms in equations (25)–(28) in the following way

$$A_{MD}^{(n)} X_{MD} \longrightarrow \sum_{i \in MD-type} A_{i,MD}^{(n)} X_{i,MD} \qquad (29)$$

and

$$A_{MD}^{(p)} X_{MD} \longrightarrow \sum_{i \in MD-type} A_{i,MD}^{(p)} X_{i,MD}, \qquad (30)$$

where the summation is over all MD excitons which can interact with deep states via the EA process.

3. Results and discussion

In order to show a usefulness of the presented model, we will compare it with experimental results from the literature. Although the EA mechanism via deep states has been discussed for 2D transition metal dichalcogenides [21], an experimental evidence of this effect has not been clearly identified in such systems. However, we can assume that both the SRH and the EA processes can coexist together with other recombination mechanisms. Thus, the comparison between the model and the experimental recombination results obtained for MoS_2 monolayer [25] will be demonstrated.

In this experiment [25], the cw source of light has been used for the illumination which means that the steady-state conditions have been created. The applied wavelength (514 nm) is associated with the photon energy of 2.41 eV, which is greater than an optical energy band-gap (counting to the first bright excitonic level) and is also greater than an energetic distance to the Rydberg excitonic states [26]. Therefore, it has been assumed that the photons excite electrons directly to the exciton continuum (the conduction band for separated charge

carriers). For this case, the steady-state generation rate of electrons (G_n) is equal to the sum of recombination rates for these carriers [25]

$$G_n = R_{SRH} + R_R + R_A = An + Bn^2 + Cn^3, \qquad (31)$$

where R_{SRH}, R_R and R_A denote the SRH, the radiative and the Auger recombination rates, respectively, whereas A represents the SRH monomolecular recombination coefficient, B is the radiative bimolecular recombination coefficient and C denotes the Auger trimolecular recombination coefficient. Here $G_n = G_{opt}$, where G_{opt} is the overall optical generation rate.

We should remind that the concentration of electrons after illumination of a material can be expressed as $n = n_0 + \Delta n$, where n_0 denotes the concentration of electrons in the conduction band under the equilibrium conditions and Δn represents an amount of electrons generated by incident photons. For the case of a strong illumination, we can assume that $n_0 \ll \Delta n$, so $n \simeq \Delta n$.

It is easy to show that the total carrier lifetime for electrons τ_n (called the overall lifetime in [25]) can be found from an expression

$$\frac{1}{\tau_n} = \frac{1}{\tau_{SRH}} + \frac{1}{\tau_R} + \frac{1}{\tau_A}, \qquad (32)$$

where the SRH lifetime is given by $\tau_{SRH} = 1/A$, the radiative lifetime can be written as $\tau_R = 1/(Bn)$ and the Auger lifetime is represented by $\tau_A = 1/(Cn^2)$.

However, we think that the excitons formation should not be neglected for 2D layers. Therefore, our aim is to enhance the above interpretation of experimental results by including the generation and recombination excitonic effects with the coexistence of both the SRH and the EA mechanisms. Thus, if we consider a direct excitation of electrons to the conduction band, the kinetic equations for electrons and excitons look as follows

$$\frac{dn}{dt} = G_{opt} - G_{n,B} - G_{n,SD} - G_{n,MD} - R_R - R_A - U_n = 0, \qquad (33)$$

$$\frac{dX_B}{dt} = G_{n,B} - R_B - E_{cap}^B - H_{cap}^B - G_{B,SD} - G_{B,MD} = 0, \qquad (34)$$

$$\frac{dX_{SD}}{dt} = G_{n,SD} - R_{SD} - E_{cap}^{SD} - H_{cap}^{SD} + G_{B,SD} = 0 \qquad (35)$$

and

$$\frac{dX_{MD}}{dt} = G_{n,MD} - R_{MD} - E_{cap}^{MD} - H_{cap}^{MD} + G_{B,MD} = 0. \qquad (36)$$

Here, the excited electrons relax non-radiatively to lower excitonic states and create bright excitons, SD excitons and MD excitons with the rates $G_{n,B}$, $G_{n,SD}$ and $G_{n,MD}$, respectively. The separated electrons can recombine via the radiative (R_R) and the Auger (R_A) processes. In addition, the SRH recombination with the EA effect occurs with the rate U_n. We should note that the SRH recombination coefficient $R_{SRH} =$

$E_{cap} - E_{em}$ is included in U_n. The capture of carriers from excitons via deep states takes place for all types of excitons. The excitonic states can also relax to ground states with the rates R_B, R_{SD} and R_{MD} for bright excitons, SD excitons and MD excitons, respectively. In addition, we should consider the formation of SD excitons and MD excitons directly from bright excitons with the rates $G_{B,SD}$ and $G_{B,MD}$, respectively.

After a simple derivation, we obtain

$$G_{opt} = R_{SRH} + R_R + R_A + R_B + R_{SD} + R_{MD}$$
$$+ E_{cap}^B + E_{cap}^{SD} + E_{cap}^{MD}. \qquad (37)$$

In general, concentrations of electrons and all types of excitons are not the same. However, we can estimate the overall effective lifetime in the form

$$\frac{1}{\tau_{eff}} \sim \frac{1}{\tau_n} + \frac{1}{\tau_X} + \frac{1}{\tau_{E_{cap}^X}}. \qquad (38)$$

Here, the total excitonic recombination lifetime τ_X can be found from equation $1/\tau_X = 1/\tau_{X_B} + 1/\tau_{X_{SD}} + 1/\tau_{X_{MD}}$, where τ_{X_B}, $\tau_{X_{SD}}$ and $\tau_{X_{MD}}$ represent the recombination lifetimes for bright excitons, SD excitons and MD excitons, respectively. The time $\tau_{E_{cap}^X}$ describes the total lifetime of electrons capture processes from excitons via deep states. It is given by $1/\tau_{E_{cap}^X} = 1/\tau_{E_{cap}^B} + 1/\tau_{E_{cap}^{SD}} + 1/\tau_{E_{cap}^{MD}}$, where the lifetimes for the capture of electrons from bright excitons, SD excitons and MD excitons can be expressed as $\tau_{E_{cap}^B} = 1/[A_B^{(n)}N_t(1-f)]$, $\tau_{E_{cap}^{SD}} = 1/[A_{SD}^{(n)}N_t(1-f)]$ and $\tau_{E_{cap}^{MD}} = 1/[A_{MD}^{(n)}N_t(1-f)]$, respectively.

The total concentration of excitons is given by $X = X_B + X_{SD} + X_{MD}$. The relation between the concentration of charge carriers and the total concentration of excitons X can be found from the Saha equation [27]

$$\frac{np}{X} = \left(\frac{\mu_X kT}{2\pi\hbar^2}\right)^{\frac{d}{2}} \exp\left(-\frac{E_B}{kT}\right), \qquad (39)$$

where the factor $d = 2$ is for 2D materials and $d = 3$ for 3D structures, E_B represents the binding energy of excitons and $\hbar$ denotes the Planck's constant divided by 2π. The reduced mass of exciton μ_X can be calculated from equation $\mu_X = m_n m_p/(m_n + m_p)$, where m_n and m_p are effective masses of electrons and holes, respectively.

For 2D monolayers, all physical quantities are usually expressed in 2D units. However, in the Salehzadeh *et al* paper [25], the generation rate G_{opt} has been calculated for a 3D volume. Therefore, the recombination coefficients A, B and C from equation (31) have been also determined in 3D units. Thus, in order to compare the presented model with these experimental results, we will use 3D units for all quantities. As a consequence, the dimensional factor in the Saha equation was chosen as $d = 3$.

Figure 2 shows the lifetimes of different processes drawn as a function of the excitation power, which is linearly proportional to the optical generation rate G_{opt}. The experimental data of the radiative lifetime τ_R, the Auger lifetime τ_A, the SRH lifetime τ_{SRH} and the total carrier lifetime τ_n are taken from figure 4 in [25]. These results were obtained for the
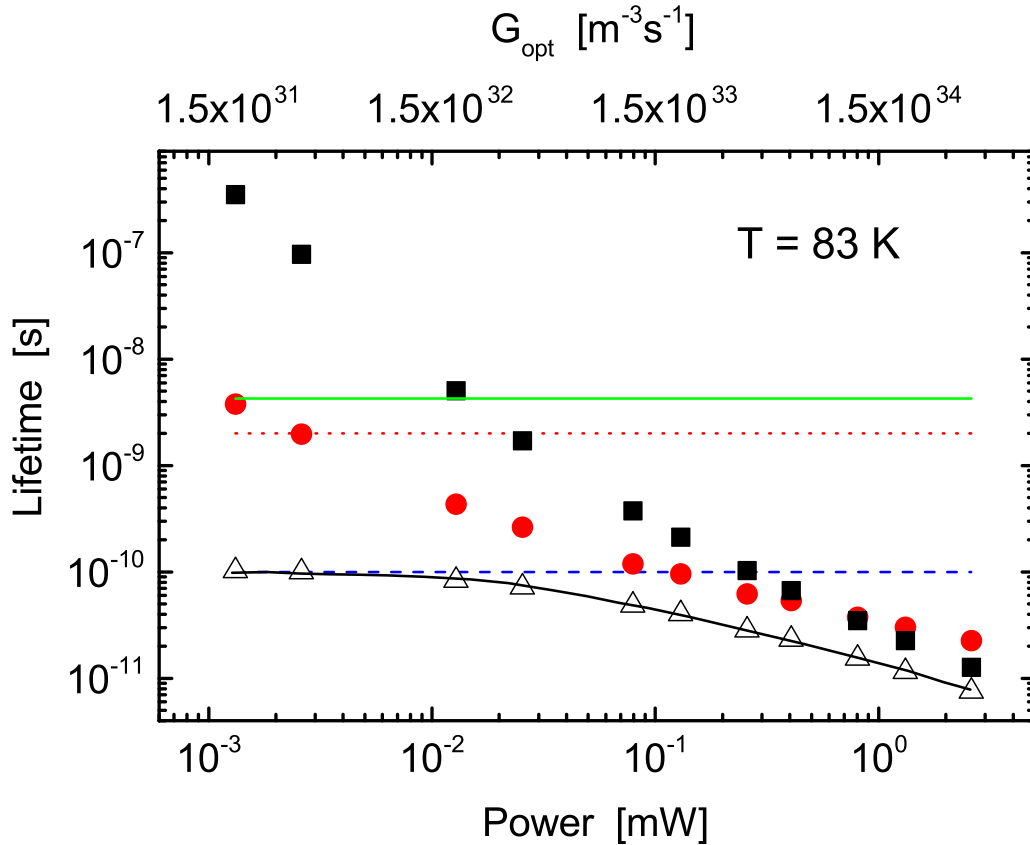
Figure 2. The lifetimes as a function of the excitation power which is proportional to the optical generation rate. Results are given for the temperature 83 K. The black closed squares, the red closed circles, the blue dashed line and the black solid line denote the experimental values of τ_A, τ_R, τ_{SRH} and τ_n, respectively. These data are taken from [25]. The green solid line, the red dotted line and the black open triangles show $\tau_{E_{cap}^X}$, τ_X and τ_{eff}, respectively. The values of all parameters are written in main text.

temperature 83 K. We have calculated the concentrations of charge carriers for different values of the generation rate from equations (31) and (32) and used them to find the total concentrations of excitons from the Saha equation (39). The exciton binding energy was taken as $E_B = 0.22$ eV [28] for all types of excitons. The effective masses of charge carriers are $m_n = 0.49 m_e$ and $m_p = 0.52 m_e$ [29], where m_e represents the mass of a free electron. In order to get reasonable parameters, the calculated lifetime of SRH recombination ($\tau_{SRH} = n/U_{SRH}$) should be the same as the experimental lifetime. We obtained $N_t = 1.3 \times 10^{22}$ m^{-3}, $N_c = N_v = 3 \times 10^{24}$ m^{-3} and $C_n = C_p = 1.4 \times 10^{-12}$ m^3 s^{-1}. The energy band-gap for separated electrons has been taken as $E_g = 2.4$ eV, which is greater than an energetic distance to the Rydberg excitonic states [26]. The position of E_t is in the middle of this band-gap.

In general, all coefficients associated with the carriers captures from excitons can have different values. However, there are still no experimental results of these parameters for 2D structures. Thus, for a simplicity, we can assume that all these coefficients are the same $A_B^{(n)} = A_{SD}^{(n)} = A_{MD}^{(n)} = A_B^{(p)} = A_{SD}^{(p)} = A_{MD}^{(p)} = 1.2 \times 10^{-14}$ m^3 s^{-1}. It has been shown experimentally [29] that the intrinsic radiative recombination time for excitons is 1.8×10^{-12} s for $T = 7$ K and the effective radiative lifetime is 2.5×10^{-9} for $T = 125$ K. Therefore, we can assume that

$\tau_X = 2 \times 10^{-9}$ s for 83 K. The green solid line and the red dotted line seen in figure 2 show the lifetimes $\tau_{E_{cap}^X}$ and τ_X, respectively. Knowing them, we could determine the overall effective lifetime from the relation (38). It is clearly visible that τ_{eff} is in an excellent agreement with the experimental total carrier lifetime for electrons τ_n.

We should note that, in general, all recombination coefficients for charge carriers and excitons are not constant. Their values can depend on the temperature, the excitation density or the type of a material. In the following, we will study the influence of temperature. Figure 3 illustrates the lifetimes associated with different processes presented as a function of the excitation power (the optical generation rate G_{opt}) drawn for two temperatures 223 K and 373 K. The experimental values of τ_n are taken from figure S4 in supporting information of paper [25]. The charge carriers recombination lifetimes τ_R and τ_A were calculated from equations (31) and (32). For these calculations, we used parameters B and C taken from figure 3 (for the exciton mode A) in [25]. The τ_{SRH} was the same as for 83 K. Due to a lack of experimental results concerning the carriers captures from excitons, we can assume the temperature independent values of $\tau_{E_{cap}^X}$. The magnitudes of the total excitonic recombination lifetime τ_X have been chosen as 3.5×10^{-9} s for 223 K and 6×10^{-9} s for 373 K, which values are reasonable with the experimental observation
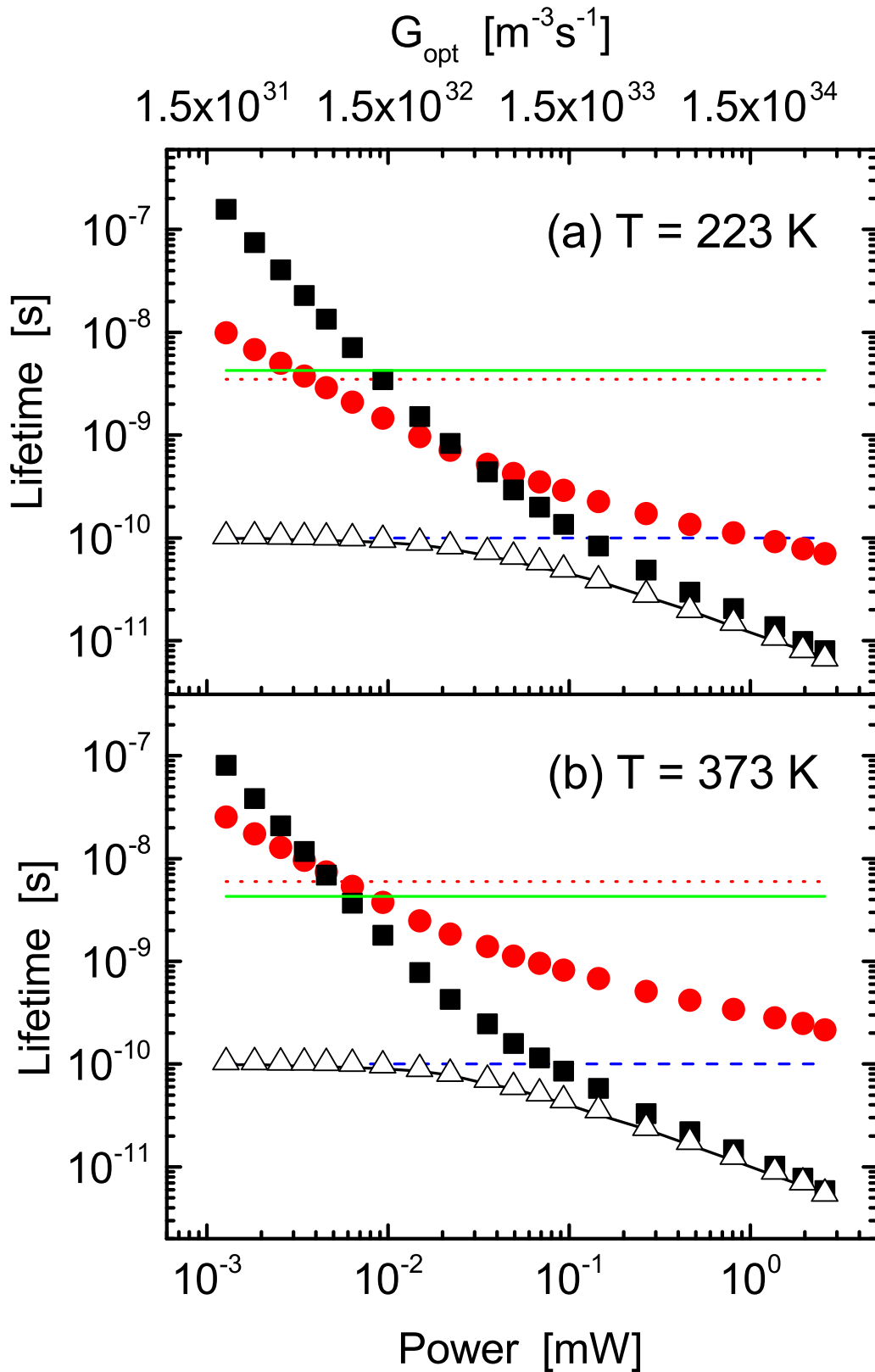
Figure 3. The lifetimes as a function of the excitation power which is proportional to the optical generation rate. Results are given for the temperatures 223 K (a) and 373 K (b). The black closed squares, the red closed circles, the blue dashed lines and the black solid lines denote the experimental values of τ_A, τ_R, τ_{SRH} and τ_n, respectively. These data are taken from [25]. The green solid lines, the red dotted lines and the black open triangles show $\tau_{E_{cap}^X}$, τ_X and τ_{eff}, respectively. The values of all parameters are written in main text.

[29]. Figure 3 shows that we obtained a very good agreement between the calculated effective lifetime τ_{eff} and the experimental overall lifetime for electrons τ_n.

It is seen that the relation (38) does not include the effective recombination rate U. However, the derived equation (24) for this rate has a physical interpretation, which can be useful to explain experimental results. Taking into account the lifetimes from paper [25], we find that U is negative for temperatures 83 K and 223 K, whereas it is positive for 373 K. This means that the EA mechanism dominates over the SRH effect in lower temperatures and leads to a situation that more separated charge carriers are created from excitons than recombine via deep states. The change of a sign for higher temperature causes that the SRH recombination starts to play a dominant role. Thus, knowing the value of U as a function of temperature, we can determine an information about the main decay mechanism via deep traps.

Additionally, one can find a temperature-dependent relation which describes a population of bright and SD excitons. It can be written as (see supplemental material of [30])

$$X_{\text{B}} = (X_{\text{B}} + X_{\text{SD}}) \frac{\exp\left(-\frac{\Delta}{kT}\right)}{2 + 2\exp\left(-\frac{\Delta}{kT}\right)}, \tag{40}$$

where Δ represents the energy difference between bright and SD excitons. The splitting between these intravalley excitonic states has been theoretically studied for MoX_2 and WX_2 monolayers [31]. Equation (40) is a consequence of the intravalley scattering observed in 2D structures. The above expression could be useful for further detailed studies. However, it was not applied here due to an unknown relation with the population of intervalley MD excitons. The temperature dependent relative concentrations of intravalley excitons (bright and SD ones) can influence on the EA process. Therefore, it should also impact on the temperature dependence of the rate U.

The other important recombination channel is an exciton–exciton annihilation, which can occur in 2D transition metal dichalcogenides [32, 33]. However, this effect takes place without trap states. Thus, it does not change the final expression of the recombination rate U. In addition, the influence of this annihilation mechanism is also neglected for the effective lifetime τ_{eff}. For the steady state case (when all derivatives over time are zero), the terms associated with this process cancel each other out in kinetic equations. Therefore, the annihilation lifetime is not included in the relation (38).

4. Summary

We have formulated the theoretical model which describes the EA recombination via deep states with a coexistence of the trap-assisted recombination in 2D monolayer materials. The impact of bright and dark excitons on the recombination rate has been taken into account. The explanation of this effect can be useful to describe photoelectrical and excitonic processes in optoelectronic and photonic devices based on 2D structures, like transition metal dichalcogenides and perovskites.

Data availability statement

The data that support the findings of this study are available upon reasonable request from the authors.

Conflicts of interest

The authors declare no conflicts of interest.

ORCID iD

Jędrzej Szmytkowski   https://orcid.org/0000-0002-6494-1307

References

[1] Moody G, Schaibley J and Xu X 2016 Exciton dynamics in monolayer transition metal dichalcogenides *J. Opt. Soc. Am.* B **33** C39–C49

[2] Wang Y, Nie Z and Wang F 2020 Modulation of photocarrier relaxation dynamics in two-dimensional semiconductors *Light Sci. Appl.* **9** 192

[3] Mueller T and Malic E 2018 Exciton physics and device application of two-dimensional transition metal dichalcogenide semiconductors *npj 2D Mater. Appl.* **2** 29

[4] Lindlau J *et al* 2018 The role of momentum-dark excitons in the elementary optical response of bilayer WSe₂ *Nat. Commun.* **9** 2586

[5] Brem S, Selig M, Berghaeuser G and Malic E 2018 Exciton relaxation cascade in two-dimensional transition metal dichalcogenides *Sci. Rep.* **8** 8238

[6] Malic E, Selig M, Feierabend M, Brem S, Christiansen D, Wendler F, Knorr A and Berghäuser G 2018 Dark excitons in transition metal dichalcogenides *Phys. Rev. Mater.* **2** 014002

[7] Feierabend M, Brem S and Malic E 2019 Optical fingerprint of bright and dark localized excitonic states in atomically thin 2D materials *Phys. Chem. Chem. Phys.* **21** 26077–83

[8] Feierabend M, Brem S, Ekman A and Malic E 2021 Brightening of spin- and momentum-dark excitons in transition metal dichalcogenides *2D Mater.* **8** 015013

[9] Liu E, van Baren J, Liang C-T, Taniguchi T, Watanabe K, Gabor N M, Chang Y-C and Lui C H 2020 Multipath optical recombination of intervalley dark excitons and trions in monolayer WSe₂ *Phys. Rev. Lett.* **124** 196802

[10] Gan Z *et al* 2019 Transient energy reservoir in 2D perovskites *Adv. Opt. Mater.* **7** 1900971

[11] Folpini G, Cortecchia D, Petrozza A and Kandada A R S 2020 The role of dark exciton reservoir in the luminescence efficiency of two-dimensional tin iodide perovskites *J. Mater. Chem.* C **8** 10889–96

[12] Mondal N, De A, Seth S, Ahmed T, Das S, Paul S, Gautam R K and Samanta A 2021 Dark excitons of the perovskites and sensitization of molecular triplets *ACS Energy Lett.* **6** 588–97

[13] Chen K *et al* 2017 Experimental evidence of exciton capture by mid-gap defects in CVD grown monolayer MoSe₂ *npj 2D Mater. Appl.* **1** 15

[14] Shockley W and Read J W T 1952 Statistics of the recombinations of holes and electrons *Phys. Rev.* **87** 835–42

[15] Hall R N 1952 Electron–hole recombination in germanium *Phys. Rev.* **87** 387

[16] Wang H, Zhang C and Rana F 2015 Ultrafast dynamics of defect-assisted electron–hole recombination in monolayer MoS₂ *Nano Lett.* **15** 339–45

[17] Li L and Carter E A 2019 Defect-mediated charge-carrier trapping and nonradiative recombination in WSe$_2$ monolayers *J. Am. Chem. Soc.* **141** 10451–61

[18] Moody G, Tran K, Lu X, Autry T, Fraser J M, Mirin R P, Yang L, Li X and Silverman K L 2018 Microsecond valley lifetime of defect-bound excitons in monolayer WSe$_2$ *Phys. Rev. Lett.* **121** 057403

[19] Fossum J G, Mertens R P, Lee D S and Nijs J F 1983 Carrier recombination and lifetime in highly doped silicon *Solid-State Electron.* **26** 569–76

[20] Hangleiter A 1987 Nonradiative recombination via deep impurity levels in silicon: experiment *Phys. Rev.* B **35** 9149–61

[21] Wang H, Strait J H, Zhang C, Chan W, Manolatou C, Tiwari S and Rana F 2015 Fast exciton annihilation by capture of electrons or holes by defects via Auger scattering in monolayer metal dichalcogenides *Phys. Rev.* B **91** 165411

[22] Danovich M, Zólyomi V, Fal'ko V I and Aleiner I L 2016 Auger recombination of dark excitons in WS$_2$ and WSe$_2$ monolayers *2D Mater.* **3** 035011

[23] Szmytkowski J 2020 A simple model of the trap-assisted recombination with the excitonic Auger mechanism *Eur. Phys. J. Plus* **135** 37

[24] Szmytkowski J 2020 Enhanced trap-assisted recombination in organic semiconductors *Solid State Commun.* **321** 114044

[25] Salehzadeh O, Tran N H, Liu X, Shih I and Mi Z 2014 Exciton kinetics, quantum efficiency and efficiency droop of monolayer MoS$_2$ light-emitting devices *Nano Lett.* **14** 4125–30

[26] Vaquero D, Clerico V, Salvador-Sánchez J, Martín-Ramos A, Diaz E, Domínguez-Adame F, Meziani Y M, Diez E and Quereda J 2020 Excitons, trions and Rydberg states in monolayer MoS$_2$ revealed by low-temperature photocurrent spectroscopy *Commun. Phys.* **3** 194

[27] Simbula A *et al* 2021 Polaron plasma in equilibrium with bright excitons in 2D and 3D hybrid perovskites *Adv. Opt. Mater.* **9** 2100295

[28] Park S, Mutz N, Schultz T, Blumstengel S, Han A, Aljarb A, Li L-J, List-Kratochvil E J W, Amsalem P and Koch N 2018 Direct determination of monolayer MoS$_2$ and WSe$_2$ exciton binding energies on insulating and metallic substrates *2D Mater.* **5** 025003

[29] Robert C *et al* 2016 Exciton radiative lifetime in transition metal dichalcogenide monolayers *Phys. Rev.* B **93** 205423

[30] Zhang X-X, You Y, Zhao S Y F and Heinz T F 2015 Experimental evidence for dark excitons in monolayer WSe$_2$ *Phys. Rev. Lett.* **115** 257403

[31] Echeverry J P, Urbaszek B, Amand T, Marie X and Gerber I C 2016 Splitting between bright and dark excitons in transition metal dichalcogenide monolayers *Phys. Rev.* B **93** 121107(R)

[32] Kumar N, Cui Q, Ceballos F, He D, Wang Y and Zhao H 2014 Exciton–exciton annihilation in MoSe$_2$ monolayers *Phys. Rev.* B **89** 125427

[33] Sun D, Rao Y, Reider G A, Chen G, You Y, Brezin L, Harutyunyan A R and Heinz T F 2014 Observation of rapid exciton–exciton annihilation in monolayer molybdenum disulfide *Nano Lett.* **14** 5625–9